Remote Sensing of Environment 213 (2018) 92–103

Contents lists available at ScienceDirect

Remote Sensing of Environment

journal homepage: www.elsevier.com/locate/rse

Detection of seagrass scars using sparse coding and morphological filter

E. Oguslu[a], Kazi Islam[e], Daniel Perez[d], V.J. Hill[b], W.P. Bissett[c], R.C. Zimmerman[b], J. Li[e,*]

[a] Department of Electronics and Communications, Turkish Air Force NCO Vocational College, Gaziemir, Izmir, Turkey
[b] Department of Ocean, Earth and Atmospheric Sciences, Old Dominion Univ., Norfolk, VA 23529, USA
[c] Florida Environmental Research Institute, Tampa, FL 33611, USA
[d] Department of Modelling, Simulation & Visualization Engineering, Old Dominion Univ., Norfolk, VA 23529, USA
[e] Department of Electrical and Computer Engineering, Old Dominion Univ., Norfolk, VA 23529, USA

ARTICLE INFO

Keywords:
Remote sensing
Sparse coding
Seagrass scar detection

ABSTRACT

The proximity of seagrass meadows to centers of human activity makes them vulnerable to a variety of habitat degrading insults. Physical scarring has long been recognized as an important but difficult-to-quantify source of habitat fragmentation and seagrass loss. We present a pixel-based algorithm to detect seafloor propeller seagrass scars in shallow water that promises to automate the detection and measurement of scars across the submarine landscape.[1] We applied the algorithm to multispectral and panchromatic images captured at the Deckle Beach, Florida using the WorldView-2 commercial satellite. The algorithm involves four steps using spectral and spatial information from radiometrically calibrated multispectral and panchromatic images. First, we fused multispectral and panchromatic images using a principal component analysis (PCA)-based pan-sharpening method to obtain multispectral pan-sharpened bands. In the second step, we enhanced the image contrast of the pan-sharpened bands for better scar detection. In the third step, we classified the contrast enhanced image pixels into scar and non-scar categories based on a sparse coding algorithm that produced an initial scar map in which false positive scar pixels were also present. In the fourth step, we applied post-processing techniques including a morphological filter and local orientation to reduce false positives. Our results show that the proposed method may be implemented on a regular basis to monitor changes in habitat characteristics of coastal waters.

1. Introduction

Seagrasses (marine angiosperms) inhabit the shallow coastal waters of temperate and tropical seas throughout the world. They provide a critical habitat and food source for a variety of wildlife, improve water quality, stabilize coastal sediments and represent an important reservoir of organic carbon (blue carbon) in the oceans (Larkum et al., 2006). However, seagrasses are particularly vulnerable to human impacts that have created a global crisis in terms of their long-term sustainability (Orth et al., 2006). Along heavily populated coasts including the Chesapeake Bay, Florida Keys and Gulf of Mexico in the United States, mechanical damage from propeller scars caused by recreational and commercial boats operating in very shallow water can have significant effects on seagrass distributions and ecosystem function (Bell et al., 2002; Kenworthy et al., 2002; Orth et al., 2002). It can take years for the scars to disappear and they often accelerate seagrass loss by facilitating erosion at scar boundaries (Zieman, 1976; Dawes et al., 1997).

Scar abundance in seagrass meadows has been assessed historically by visual assessment of uncalibrated aerial photography (RGB) that provide semi-quantitative estimates of the areal coverage of disturbed patches in a given meadow (Sargent et al., 1995; Dunton and Schonberg, 2002; Madley et al., 2004; Hallac et al., 2008; Orth et al., 2017). Polygons delineating scarred habitat are often outlined by hand using interactive GIS software and then rated as being lightly, moderately or severely scarred, based on visual inspection. This approach has proved useful for relating the relative intensity of seagrass scarring with other factors such as proximity to shorelines, navigation channels, recreational fishing grounds and water depth using regression techniques (Hallac et al., 2008). Although useful for predicting vulnerability of particular environment and potential management responses, these approaches remain labor intensive, both in terms of image acquisition and analysis that inhibit routine application for monitoring physical change to seagrass meadows in shallow waters or time series assessment of management strategy effectiveness.

There are many challenges for accurate, automated propeller scar detection and quantification. Firstly, propeller scars can have different shapes including straight lines, smooth curves, circles and ellipses.

* Corresponding author.
E-mail address: jli@odu.edu (J. Li).

[1] A preliminary version of the paper was presented at the SPIE Remote Sensing Conference, Amsterdam, Netherlands, 2014 (Oguslu et al., 2014).

https://doi.org/10.1016/j.rse.2018.05.009
Received 22 October 2016; Received in revised form 3 May 2018; Accepted 4 May 2018

Secondly, propeller scars can also have various lengths and widths that change over time and with seafloor bathymetry. Thirdly, although propeller scars are usually defined as bright quasi-linear regions surrounded by dark vegetation, they can sometimes appear as dark lines in very shallow water, particularly at low tide when adjacent seagrass leaves or drifting algae fill the scar depressions. Finally, naturally occurring patches of bare sediment on the seabed can be as bright as the propeller scars. All of these variations pose significant challenges for automatic detection and quantification of propeller scars amid the background "noise" of naturally occurring bright and dark patches distributed across the seafloor. Green and Lopez (2007) and Green et al. (2011) were the first to utilize automated techniques for propeller scar detection from pan-sharpened multispectral airborne imagery using an object-oriented classification scheme that consisted of field investigations, image segmentation software, and classification and regression tree analysis. The method, however, still required some manual editing, field observations and injection of the classification rules to obtain final detection results that may not translate to other locations without additional rounds of ground-truth and calibration. Further, Critical needs for proper tidal stage, wind and surface wave conditions, sun angle, clouds and haze limit the ability of airborne systems to provide image data on a routine basis.

The goal of this study, was to develop an automated sparse coding algorithm to detect both bright and dark propeller scars from high resolution (0.3 m) orbital (satellite) imagery as a pathway for routine acquisition, analysis and environmental monitoring. We focused on pan-sharpened images obtained from WorldView-2, a commercial satellite operated by DigitalGlobe, Inc. The sparse coding approach has proved to be particularly useful for image classification by sparsely representing different image patches (e.g., propeller scars vs. randomly occurring patches) differently using an image dictionary (Coates and Ng, 2011; Soltani-Farani et al., 2015). The development of an automated system for detection and quantification of propeller scars from high spatial resolution satellite imagery promises to be a valuable tool for managing seagrass meadows and other important resources in shallow coastal environments exploited by recreational and commercial activities.

2. Materials and methods

2.1. Remote sensing data and preprocessing

Panchromatic and multispectral images were captured in May 2010 near Deckle Beach, Florida (FL), USA by WorldView-2 (WV-2), an orbiting multispectral imaging system operated by DigitalGlobe, LLC. Using a specific tasking assignment, we obtained images with an off-nadir view of 20–37°, and a target azimuth angle range at 307 degrees (true solar zenith angle of 127 + 180°) plus/minus 45 degrees (or between 262 and 352°). The WV-2 imaging instrument contains a panchromatic band with high spatial resolution (PAN; 0.46 m at nadir viewing) and eight multi-spectral bands with lower spatial resolution (1.84 m at nadir viewing). The four primary multi-spectral bands include traditional blue, green, red and near-infrared bands. Four additional bands include a shorter wavelength blue band, centered at approximately 427 nm, called the coastal band for its applications in water color studies; a yellow band centered at approximately 608 nm; a red edge band centered strategically at approximately 724 nm at the onset of the high reflectivity portion of above-water vegetation response; and an additional, longer wavelength near infrared band, centered at approximately 908 nm, which is sensitive to atmospheric water vapor.

The multispectral image was delivered in six separate tiles that were georeferenced and placed in a mosaic to yield a single image file with eight separate spectral bands plus the panchromatic band. No atmospheric correction was performed on the panchromatic band. Atmospheric correction of the multispectral image was performed using the empirical line method in which the spectral return from the Digital Globe image was matched to in situ measurements made on the same day at 22 stations across the image by a survey boat. At each station, two floating spectroradiometer systems were utilized in tandem to measure downwelling spectral irradiance [$E_s(0^+)$] above the sea surface (395 to 795 nm, 2.5 nm bandwidth), upwelling spectral radiance 0.65 m beneath the sea surface [$L_u(0.65, \lambda)$, HTSRB, Satlantic Instr.], and upwelling irradiance and radiance 0.21 m beneath the sea surface [$E_u(0.21)$, $L_u(0.21)$, respectively, HyperPro, Satlantic Instr.]. The spectral upwelling diffuse attenuation coefficient [$K_{Lu}(\lambda)$] was calculated from $L_u(0.65, \lambda)$ and $L_u(0.21, \lambda)$ measured as:

$$K_{Lu} = -\frac{1}{z}\ln\frac{L_u(0.65)}{L_u(0.21)} \tag{1}$$

where z was the difference in depth between the sensors placed at 0.65 and 0.21 m (0.44 m). Upwelling radiance just beneath the air-water interface [Lu(0-, λ)] was calculated using $K_{Lu}(\lambda)$ to propagate Lu (0.21, λ) to the surface using Beers Law (Kirk, 1994). A factor of 0.54 was then used to extrapolate Lu(0−, λ) across the air-water interface [Lw (0+, λ)] (Morel and Mueller, 2003). Remote sensing reflectance [Rrs(λ)] was then computed as Lw (0+, λ)/Es(0+, λ). Spectral resolution of the field measurements was reduced to match the spectral bands of the WV-2 image based on the published spectral response functions (www.digitalglobe.com). We then performed a linear regression between the 22 in situ measurements their corresponding WV-2 spectra at the same locations to create the gain and offset for each band that effectively removed atmospheric signals from the image.

Propeller scars in the seagrass meadow were visibly present in the panchromatic image (Fig. 1) and in the in the third to sixth bands (green, yellow, red, red edge bands). The pan-sharpened data set was created by fusing the panchromatic image with the four multispectral bands using a PCA-based pan-sharpening method (Shettigara, 1992) as described below. The model was trained using a 720 by 820 pixel segment located near Hagen's Cove Park, FL that contained numerous propeller scars (Fig. 1).

2.2. Algorithm development

To overcome the challenges of distinguishing propeller scars from the surrounding clutter of light and dark patches, we developed an automatic system using a sparse coding method consisting of four steps

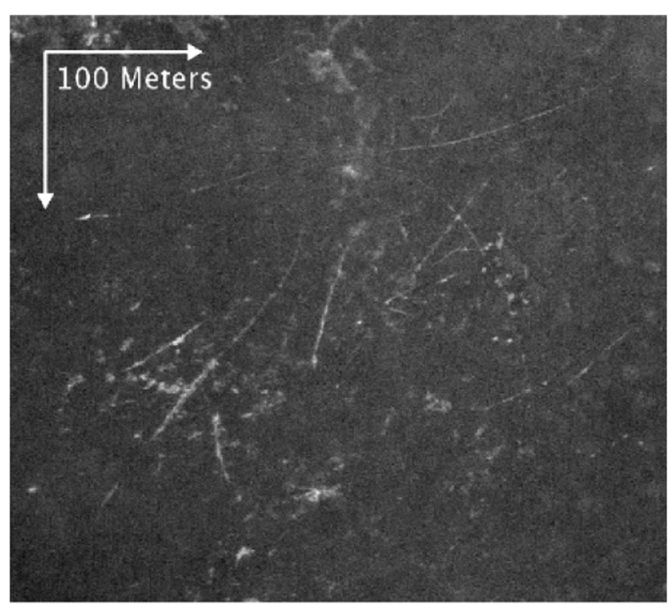

Fig. 1. Panchromatic image obtained over shallow vegetated area near Hagen's Cove Park.